2014 IEEE International Conference on Robotics & Automation (ICRA)
Hong Kong Convention and Exhibition Center
May 31 - June 7, 2014. Hong Kong, China

A robust landing and sliding maneuver controller for a quadrotor vehicle on a sloped incline

David Cabecinhas, Rita Cunha and Carlos Silvestre

***Abstract*— This work addresses the design and experimental evaluation of a robust controller for a quadrotor landing maneuver comprising the approach to a landing slope and sliding on that slope, before coming to a complete halt. During the critical landing flight phase the dynamics of the vehicle change with the type of contact with the ground and a hybrid automaton, whose states reflect the several dynamic behaviors of the quadrotor, is employed to model the vehicle throughout the complete maneuver. The quadrotor landing problem is broken down into separate maneuver generation and robust trajectory tracking problems, which are combined to achieve a successful maneuver that is robust to possible uncertainties. Experimental results are provided to attest the feasibility of the proposed landing procedure.**

I. INTRODUCTION

Flight control and applications of Unmanned Aerial Vehicles (UAV) is an active and challenging topic of research, with crucial importance to numerous civilian and military applications. Examples of applications can be gathered from a number of recent journal special issues dedicated to these platforms, with topics ranging from the flight control [1] and aerial robotics [2] to a plethora of remote sensing applications, such as the ones detailed in [3]. Research on autonomous UAVs has been traditionally focused on the free flight regime, where the vehicle is completely airborne and performs hover or forward flight maneuvers. However, in many envisaged working scenarios, an aerial vehicle must also perform the challenging take-off and landing maneuvers, where the vehicle is in contact with the ground and additional complications arise.

Early research work with experimental results for landing maneuvers considered horizontal flat and stable landing surfaces. The more challenging problem of landing an autonomous helicopter on an oscillating platform, such as the deck of a ship at sea, was considered in [4]. In this work the authors devise an inner-model based control solution, based on the assumption that the vertical oscillation is the result of the superposition of sinusoids of unknown amplitude, phase and frequency. More recently, a landing controller able to cope with a landing platform that is moving vertically with unknown dynamics was developed in [5], where landing is achieved based on optical flow measurements. The related problem of landing on a horizontally moving platform was studied in [6], where the authors tackle the problem of landing the vehicle resorting to an inner-outer loop control strategy with the attitude as the inner-loop reference.

Non-traditional approaches to landing have been developed in [7] and [8], where solutions for landing aerial vehicles by perching on vertical walls are studied. More recently, particular emphasis has been payed to other flight conditions where controlled interaction with the environment occurs, whether it is contact with vertical walls, the ground or even using an arm-like extension to interact with objects [9], [10]. The use of a VTOL vehicle to apply forces to the environment while maintaining flight stability was proposed in [11]. Similarly, in [9] a quadrotor vehicle is fitted with an arm, which is used to interact with the environment. Further exploration of flight modes were physical contact with the environment occurs as can be found in [12], which focuses on the interaction of a ducted-fan aerial vehicle with a vertical surface, where sliding is allowed.

In this paper, we build on the ideas developed in [13] and [10] and propose a hybrid flight controller that ensures a successful completion of a landing maneuver, from a free flight configuration to a complete halt, for a quadrotor vehicle in challenging circumstances. In the spirit of [13], a hybrid automata is used to model the vehicle, thereby encapsulating the complete dynamics of the different flight regimes it must transverse. Once the hybrid automaton is defined, the landing problem is addressed as a combination of trajectory generation and trajectory tracking control problems. In particular, both the reference signals and the feedback laws for each operating mode are derived considering explicitly the presence of uncertainties. The references are designed such that their practical, and not perfect, tracking ensures that the desired transitions happen, despite the possible presence of uncertainties.

II. PROBLEM STATEMENT

The main objective of the paper is the development of a controller for an aircraft that robustly ensures a successful completion of a landing maneuver on an inclined plane, from a free flight configuration to a complete halt. A control solution is proposed for a quadrotor vehicle actuated in force, generated by the propellers, allowing for full torque control and generating a total force aligned this the propeller direction. The full state of the quadrotor is assumed to be known and available for feedback by controller.

A quadrotor aircraft is actuated in force, generated by the four propellers, and possesses hover and VTOL (vertical

This work was supported by project FCT PEst-OE/EEI/LA0009/2013 and by project FCT SCARVE (PTDC/EEA-CRO/102857/2008).

The authors are with the Department of Electrical Engineering and Computer Science, and Institute for Robotics and Systems in Engineering and Science (LARSyS), Instituto Superior Técnico, Universidade Técnica de Lisboa, 1049-001 Lisboa, Portugal. D. Cabecinhas and C. Silvestre are also with the Department of Electrical and Computer Engineering, Faculty of Science and Technology of the University of Macau.

takeoff and landing) capabilities. In this work, for sake of simplicity, we consider only the *planar dynamics* on the configuration manifold $\mathbb{S}^1 \times \mathbb{R}^2$. Fig. 1(a) presents a graphical description of the quadrotor geometry and the landing environment. The landing ground is modeled as a flat surface at an angle β with the horizontal. A body-fixed frame $\{\mathcal{B}\} = \{CM, \vec{j_B}, \vec{k_B}\}$ is attached to the quadrotor's center of mass (CM), with the vector $\vec{k_B}$ pointing upward, along the thrust direction. The inertial frame $\{\mathcal{I}\} = \{O, \vec{j}, \vec{k}\}$ is defined by the vectors $\vec{j}$ and $\vec{k}$ that point North and up, respectively. An additional frame $\{\mathcal{L}\} = \{O, \vec{j_L}, \vec{k_L}\}$ is attached to the origin of $\{\mathcal{I}\}$ and rotated with respect to $\{\mathcal{I}\}$ by an angle β. The angle θ denotes the rotation angle from the inertial frame to the body frame. The planar model of the quadrotor, illustrated in Fig. 1(b), has two counter-rotating motors for propulsion, generating the aerodynamic forces F_1 and F_2, and a landing gear with two points of contact with the ground, denoted by A and B. The distance from the center of mass to each motor and to each contact point are denoted by r and ℓ, respectively. The angle with vertex in CM and subtended by the motor and contact point is denoted by γ. The shorthand $\ell_g = \ell \cos(\gamma)$ is introduced to simplify mathematical expressions.

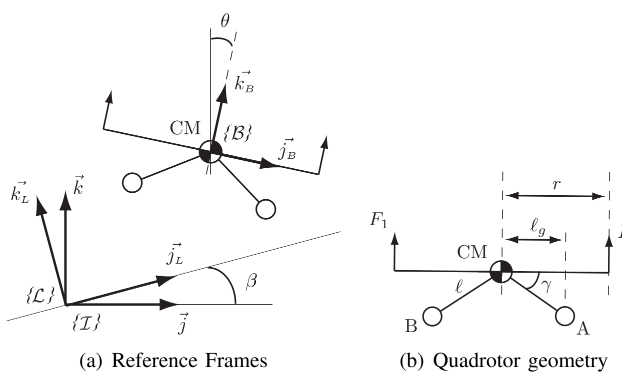

Fig. 1. Take-off slope and quadrotor

III. Quadrotor Hybrid Model

The quadrotor is modeled as a hybrid automaton with five operating modes, corresponding each mode to the different dynamics that the vehicle is subject to. The modes are distinguished by the number of contact points of the landing gear with the ground and the existence of relative movement between the contact point and the ground. In the *Free Flight* (FF) mode, the quadrotor is in free flight and no contact with the landing slope occurs. The operating modes *Take-off-and-Landing* (TL and TLs) denote a take-off or landing situation where there exists a single contact point between the quadrotor and the ground. The shorthand notation TL denotes the non-sliding situation and TLs the take-off-and-landing mode where sliding exists between the quadrotor and the ground. Lastly, the *Landed* (LL and LLs) operating mode corresponds to having the landing gear in full contact with the ground, with both points A and B touching the landing slope. Likewise, we denote by LL the non-sliding situation and by LLs the landing operative mode where the quadrotor slides on the ground. The coordinates of CM in the $\{\mathcal{I}\}$ reference frame are denoted by (x, z) and the coordinates of the contact point A expressed in the $\{\mathcal{L}\}$ frame are denoted by (α, ζ). To simplify the mathematical descriptions of the various quadrotor dynamics, the state of the quadrotor is expressed in different coordinate systems, according to its operative mode.

A. Hybrid model of the quadrotor dynamics

A description of the overall quadrotor dynamics is obtained by means of a hybrid automaton whose states correspond to the different operating modes. A hybrid automaton is identified by the following objects, instanced here for the specific case of the planar quadrotor.

1) Operating Modes: The quadrotor automaton comprises the set $\mathcal{Q}$ of *operating modes*, denoted by $\mathcal{Q} = \{LL, LLs, TL, TLs, FF\}$, with the meaning *landed*, *landed sliding*, *take-off and landing*, *take-off and landing sliding*, and *free flight*, respectively.

2) Domain map: The state of the system $\xi \in \mathbb{R}^6$ is described by either $(x, \dot{x}, z, \dot{z}, \theta, \dot{\theta})$ or $(\alpha, \dot{\alpha}, \zeta, \dot{\zeta}, \theta, \dot{\theta})$ coordinates. When the UAV is in contact with the ground (LL, LLs, TL, and TLs operating modes), the preferred reference frame is $\{\mathcal{L}\}$ frame and the state described by $\xi = (\alpha, \dot{\alpha}, \zeta, \dot{\zeta}, \theta, \dot{\theta})$. For the free flight operating mode we use frame $\{\mathcal{I}\}$ and the state $\xi = (x, \dot{x}, z, \dot{z}, \theta, \dot{\theta})$.

3) Flow map: The flow map $f : \mathcal{Q} \times \mathbb{R}^6 \times \mathbb{R}^2 \to \mathbb{R}^6$ describes for each operating mode $q \in \{LL, LLs, TL, TLs, FF\}$ the evolution of the state variables. In each operating mode q we have the dynamic system

$$\dot{\xi} = f(q, \xi, u), \tag{1}$$

where each function $f(q, \xi, u)$ is derived from the differential equations that govern the movement of the quadrotor vehicle. For further detail on their definition the reader is directed to [10], where the derivation of the quadrotor dynamics for the several operating modes can be found.

4) Edges: The set of edges $\mathcal{E} \subset \mathcal{Q} \times \mathcal{Q}$ includes all the pairs (q_1, q_2) such that a transition between the modes q_1 and q_2 is possible, for some combination of state and actuation. For the take-off and landing procedures, we consider the transitions depicted in Fig. 2. Direct edges linking LL to FF or FF to LL are not modeled as these suffer from robustness issues and are not used for the maneuvers. Nonetheless, these transitions can be equivalently obtained by considering sequential instantaneous transitions through the intermediate operative modes TL and TLs.

5) Guard mapping: The set-valued guard mapping $\mathcal{G} : \mathcal{E} \rightrightarrows \mathbb{R}^6 \times \mathbb{R}^2$ determines, for each edge $(q_1, q_2) \in \mathcal{E}$, the set $\mathcal{G}(\{q_1, q_2\})$ to which the quadrotor state ξ and inputs F_1, F_2, must belong so that a transition from q_1 to q_2 can occur. There are three main groups of transitions to consider for the landing procedure. First, the operating mode transitions between free flight and the TLs operating mode depend on the force perpendicular to the slope $F_\perp$,

$$F_\perp(\theta, F_1, F_2) = (F_1 + F_2)\cos(\theta + \beta) - mg\cos\beta,$$

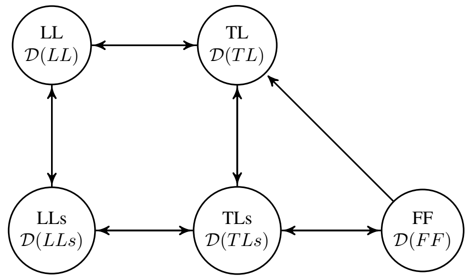

Fig. 2. Planar quadrotor hybrid automaton

and the height of the quadrotor relative to the ground. Second, the transitions where the quadrotor goes from a state with one contact point (TL and TLs operating modes) to two contact points (LL, LLs) are governed by the sign of the torque F_τ at point A,

$$F_\tau(\theta, F_1, F_2) = (F_1+F_2)l_g + (F_1-F_2)r - mg\ell\cos(\theta+\gamma),$$

and by the angle of the vehicle with the slope, $\theta+\beta$. The inverse transition depends only on the sign of F_τ. Last, we have the transitions between the *at rest* and the *sliding* modes, which are governed by the relation between the force along the slope at the contact point, the perpendicular force $F_\perp$, and the vehicle's velocity along the slope $\dot\alpha$. For the detailed expressions of the guard sets the reader is referred to [10].

6) Reset maps: For each $(q_1, q_2) \in \mathcal{E}$ and $(\xi, u) \in \mathcal{G}(\{q_1, q_2\})$, the reset map $\mathcal{R} : \mathcal{E} \times \mathbb{R}^6 \times \mathbb{R}^2 \to \mathbb{R}^6$ identifies the jump of the state variable ξ during the operating mode transition from q_1 to q_2. The only reset maps that result from physical interaction are the ones governing the transitions from FF to TLs and TL to LL. In particular, for reference trajectory generation, we model the map $\mathcal{R}(\{TL, LL\}, (\xi, u))$ under the assumption of an inelastic collision and the map $\mathcal{R}(\{FF, TLs\}, (\xi, u))$ is modeled under the assumption of inelastic impact along the perpendicular of the landing slope and by considering energy conservation – see among others [14]. This results in a trivial transition from TL to LL. The transition from Free Flight to the TLs operating mode is more complex and is analyzed in the sequel. The kinetic energy of the vehicle, ignoring the constant lateral velocity along the slope, before and after the impact is given respectively by

$$E^- = \frac{1}{2}m(\dot\alpha_{CM}^-)^2 + \frac{1}{2}m(\dot\zeta_{CM}^-)^2 + \frac{1}{2}\mathbb{J}(\dot\theta^-)^2$$

and

$$E^+ = \frac{1}{2}m(\dot\alpha_{CM}^+)^2 + \frac{1}{2}m\ell_g\cos\gamma(\theta^+)^2,$$

where $\dot\alpha_{CM}$ and $\dot\zeta_{CM}$ are the velocity components of the center of mass in the {L} frame. With $c_E \in (0, 1]$ an energy loss coefficient, it turns out that $(E^+)^2 = c_E(E^-)^2$ and then

$$\dot\theta^+ = c_E\sqrt{(\dot\zeta_{CM}^-/(\ell_g\cos\gamma))^2 + (J\dot\theta^-/(m\ell_g\cos\gamma))^2}.$$

and

$$(\dot\alpha_{CM}^+)^2 = \sqrt{c_E}(\dot\alpha_{CM}^-)^2.$$

Then by considering the constraint on ζ_{CM} characterizing $\mathcal{D}_{TL}$ and $\mathcal{D}_{TLs}$ we obtain $(\dot\zeta_{CM})^+ = \dot\theta^+\ell\cos(\theta^- + \gamma + \beta)$.

IV. Robust Control Strategy and Architecture

With the hybrid automaton in hand, the problem of performing a landing maneuver can be reformulated as a problem of changing the operative mode q from the initial free flight mode FF to the final landed configuration LL, by going through the intermediate states. The sequence of operating modes for the landing maneuver is chosen as FF, TLs, TL and finally LL, for which the transitions can be achieved robustly.

Following the general framework proposed in [13], the control problem is divided into two different steps. The first step amounts to computing, for each of the three desired transitions ($FF \to TLs$, $TLs \to TL$ and $TL \to LL$) , reference trajectories for both the states ξ and the inputs u of the system, jointly denoted as *reference maneuvers*. For each operating mode $q \in \mathcal{Q}$, the reference maneuvers are designed to guarantee robustness with respect to a design parameter $\epsilon > 0$, meaning that practical tracking of the reference trajectories, up to a tracking error ϵ (in both state and input), ensures that only the desired transition is achieved. The second step consists of designing feedback control laws for each operating mode guaranteeing that, for the proposed reference maneuvers and despite parametric uncertainties and exogenous disturbances, the tracking error (both in the state and in the input) is upper bounded by the design parameter ϵ, so that the planned transition is enforced.

A. Robust Reference Maneuvers

To precisely define the maneuvers of interest, we denote by $\upsilon_q(t) = (\xi(t), u(t))$ a maneuver taking place in the operating mode $q \in \mathcal{Q}$ and by $\operatorname{gr}\upsilon_q$ the graph of the maneuver in a certain time interval. We now present multiple straightforward robust approach trajectories whose practical following leads the quadrotor from free flight to a final landed position in a controlled manner. The maneuvers are parameterized by their starting conditions and are combined to generate the robust transition maneuvers, according to [13].

The proposed complete landing maneuver is depicted in Figure 3. The landing procedure starts in free flight, where a horizontal landing path is tracked. This eventually leads to a collision with the sloped ground, at which instant the supervisor selects the TLs controller and starts tracking a reference maneuver that leads the quadrotor to the TL state. The quadrotor then slides up the slope, tracking a TLs to TL trajectory, until it comes to a halt at a desired location. Upon coming to a halt, the quadrotor transitions to the TL operating mode mode and the supervisor uses the TL low-level controller to track a TL to LL trajectory that finally levels the quadrotor with the ground, without starting to slide again. Once all the landing gear contact points touch the ground and the final transition to the Landed mode is complete, the motors are turned off and the quadrotor remains at rest.

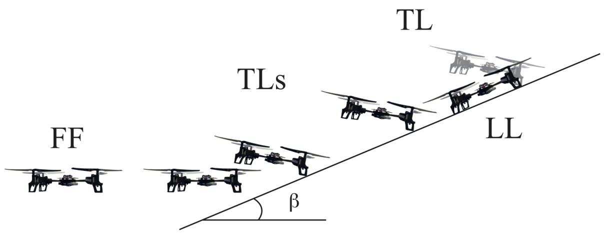

Fig. 3. Sketch of a complete quadrotor landing maneuver

1) FF → TLs robust transition maneuver: For taking the aircraft from free flight to the takeoff-and-landing sliding operating mode we propose a maneuver that leads to the quadrotor sliding up. This maneuver is chosen to have a minimal impact on the quadrotor upon touchdown on the landing slope. The quadrotor is chosen to track a horizontal line at a constant velocity until the contact point A of the landing gear touches the landing slope. For the quadrotor model at hand, the reference maneuver is defined as

$$\begin{aligned} x^\star(t) &= x_0, & \theta^\star(t) &= 0, \\ y^\star(t) &= y_0 + v_y(t - t_0), & F_1^\star(t) &= F_2^\star(t) = mg/2, \end{aligned}$$

for positive lateral velocity v_y, initial conditions x_0, $y_0 \in \mathbb{R}$ and initial time $t_0 \in \mathbb{R}$. The positive velocity corresponds to a landing maneuver where the quadrotor lands from the lower side of the slope. This maneuver ensures that only one of the quadrotor's landing gear hits the slope and that the quadrotor starts to slide on the ground, forcing a transition to the TLs mode, if tracked with an error smaller than ϵ. The time instant at which the transition occurs depends on the location of the slope, the quadrotor initial position (x_0, y_0) and the lateral approach velocity v_y.

2) TLs → TL robust transition maneuver: Following Figure 3, in the TLs operating mode the quadrotor tracks a straight line along the slope and decreases its velocity, until it comes to a halt. We define a reference maneuver with constant acceleration for the contact point and a fixed tilt angle as follows

$$\begin{aligned} \alpha^\star(t) &= \alpha_0 + v_\alpha(t - t_0) - a_\alpha(t - t_0)^2, \\ \theta^\star(t) &= \theta_0, \end{aligned}$$

for initial conditions $\alpha_0 \in \mathbb{R}$ and positive parameters v_α, a_α and θ_0. The corresponding reference inputs $F_1^\star(t)$ and $F_2^\star(t)$ are obtained by dynamic inversion of vehicle model. A set of maneuvers with different initial condition parameters at the initial time instant t_0 is considered so as to cover the whole region of possible initial conditions that arises when the tracking of the preceding maneuver is not perfect. The tilt angle θ_0 that the quadrotor follows while sliding should be slightly positive so that the quadrotor is able to slide along the slope robustly, without returning to the free flight operating mode. The transition to TL occurs when $\dot{\alpha} = 0$.

3) TL → LL robust transition maneuver: Once the quadrotor comes to a halt, the objective is to bring it to the slope level, without inducing a sliding movement again. In this operating mode we are only interested in controlling the tilt angle, for which we define the reference trajectory

$$\theta^\star(t) = \theta_0 - v_\theta t. \tag{2}$$

for a positive parameter v_θ. The quadrotor is finally leveled with the landing slope when $\theta^\star(t) = -\beta$. The reference input is determined by (2) and the reference *total thrust*, $T^\star = F_1^\star + F_2^\star$, which is chosen to converge from its initial value down to zero. In order for the maneuver to be robust, the balance between $T^\star(t)$ and $\theta^\star(t)$ must be such that the vehicle is always ϵ-far from restarting to slide during the whole transition maneuver. For the duration of this transition maneuver, the displacement of the landing gear contact point is constant, i.e. $\alpha(t) = \alpha_0$.

B. Single operating mode controllers

In this section we describe the controllers employed in each operating mode to drive the vehicle along the desired transition trajectories, in order to achieve a successful landing maneuver. These are based on previous works by the authors, namely [15] and [10], wherein locally Input-to-State-Stable (ISS) controllers (see [16] for a definition) for free flight and for the operating modes where contact occurs have been developed. Each of the controllers is required to stabilize the closed-loop system, for the appropriate dynamics, in a practical sense. From this follows that, despite possible disturbances and perturbations, the maneuver tracking error remains within a distance ϵ of the reference maneuver, therefore culminating in an successful operating mode transition.

1) Free flight controller: To steer the vehicle in free flight we use the backstepping controller developed in [15], restricted to a two dimensional setup. The state feedback controller imbues the error system with a Lyapunov function with strictly negative derivative, resulting a closed-loop system that is locally ISS with respect to the external disturbances considered for the free flight regime at the force level. As a direct consequence, there exists a maximum disturbance bound for which it can be ensured that the maneuver error is within the required limits.

2) Takeoff-and-landing controllers: The control law for the TLs dynamics is a proportional-derivative controller chosen as

$$F_\alpha(t) = -K_P(\alpha - \alpha^\star + K_D(\dot{\alpha} - \dot{\alpha}^\star)) + F_\alpha^\star(t) \tag{3a}$$

$$F_\theta(t) = -K_P(\theta - \theta^\star + K_D(\dot{\theta} - \dot{\theta}^\star)) + F_\theta^\star(t) \tag{3b}$$

where K_D, K_P are positive design parameters. The forces F_α and F_θ are generalized forces acting on the respective states (with $F_\alpha^\star(t)$ and $F_\theta^\star(t)$ the corresponding forces for the reference maneuver) and uniquely define the quadrotor's input forces $F_1(t)$ and $F_2(t)$. As shown in [10], the control parameters can be tuned so that the closed-loop trajectory remains ϵ-close to the robust reference maneuver provided that the initial error and the uncertainty in the friction coefficient are sufficiently small. A similar controller is used for the non-sliding situation where just the quadrotor angle θ is controlled through (3b), with the input forces $F_1(t)$ and $F_2(t)$

being defined uniquely defined by the additional specification of the desired resulting total force $T(t) = F_1(t) + F_2(t)$.

3) Landed mode: The landed state is the goal state of the landing maneuver. As such, in the operation mode the objective is to have the propellers of the vehicle come to a full halt, which is attained by setting both quadrotor forces to zero once the quadrotor is leveled with the landing slope, to prevent further movement. To avoid a large discontinuity in force input, we consider a maximum rate of variation for the propeller input and define the control law as

$$F_1(t) = \max(F_1(0) - \rho t, 0),$$
$$F_2(t) = \max(F_2(0) - \rho t, 0),$$

where the positive parameter ρ is the rate of variation of the thrust force.

C. Supervisor

The supervisor orchestrates the switch of the low-level controllers and drives them with the appropriate reference maneuver according to the actual state of the vehicle. In order to apply the hybrid robust control strategy, we start by designing four robust reference maneuvers $(\xi^\star_{FF}, u^\star_{FF}) : [t_{01}, t_{f1}] \to \mathcal{D}(FF)$, $(\xi^\star_{TLs}, u^\star_{TLs}) : [t_{02}, t_{f2}] \to \mathcal{D}(TLs)$, $(\xi^\star_{TL}, u^\star_{TL}) : [t_{03}, t_{f3}] \to \mathcal{D}(TL)$, $(\xi^\star_{LL}, u^\star_{LL}) : [t_{04}, t_{f4}] \to \mathcal{D}(LL)$ verifying the conditions detailed on Section IV-A for some fixed ϵ and respective operative mode. Subsequently, with the reference maneuvers and ϵ fixed, we fix the four low-level controllers according to the structures and the design principles specified in Section IV-B. Let u_{FF}, u_{TLs}, u_{TL}, u_{LL} be the control laws discussed in Section IV-B for each of the operating modes. The supervisor logic switches the low-level controller according to the actual state $q(t)$ of the vehicle. The latter takes values in the set $\{FF, TLs, TL, LL\}$ and it is supposed to be known by combining measurements from sensors, either external or appropriately placed in the quadrotor airframe. The supervisor logic is thus simply $u(t) = u_{q(t)}(t)$.

V. Experimental results

In this section we present the results for an experimental run of the proposed hybrid controller. The vehicle used for the experiments is a radio controlled Blade mQX quadrotor [17] and a VICON Bonita motion capture system [18] to obtain position and orientation measurements for the aircraft as well as an estimate for the linear velocity. The inputs for the quadrotor used in this experiment do not include each motor force individually, thereby preventing the straightforward experimental testing of the theoretical framework. To overcome this issue, the $\ddot{\theta}$ angular dynamics are integrated in simulation using the appropriate flow map (1) computed for the current quadrotor state and inputs F_1 and F_2 coming from the low level controllers. The resulting angular velocity $\dot{\theta}$ and the total thrust are then used as inputs for the physical quadrotor. This setup is depicted in Figure 4.

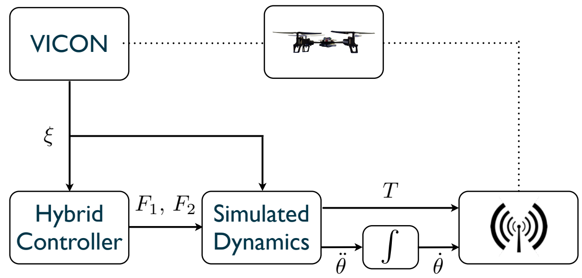

Fig. 4. Experimental setup with simulated quadrotor state.

To adapt the physical setup to a 2D control setting, the quadrotor is restricted to a vertical plane along the slope and its yaw is kept such that two of its landing gear contact points point in the slope direction, as shown in Figure 5. For the proposed maneuver, the quadrotor lands from the left to the right, relative to the figure, keeping the yaw angle such that both the right side contact points touch the slope at the same time. Landing with a correct yaw angle allows the quadrotor to tilt and continue in the same 2D plane, allowing for a good approximation of a 2D setting.

Fig. 5. Quadrotor performing a TLs to TL robust transition maneuver

The quadrotor's 2D physical parameters are $l_g = r = 0.09\,\text{m}$, $h_{CM} = 0.025\,\text{m}$, $\ell = \sqrt{l_g^2 + h_{CM}^2}$, $\gamma = 15.5°$. The landing slope has a $\beta = 20°$ incline. The friction coefficient is taken as $\mu_0 = 1$. The controller design parameters are $K_{P\theta} = 3$, $K_{D\theta} = 0.2$, $K_{P\alpha} = 0.2$, $K_{D\alpha} = 0.15$, for the TL and TLs modes local controllers.

For the landing procedure, the reference trajectory consists of a sequence of robust approach maneuvers FF→TLs, TLs→TL, and TL→LL, resulting in the vehicle sliding up the slope and coming to a halt at the desired landing point. The tracking of the quadrotor displacement and tilt angle is presented in Figures 6 and 7. The figures are divided in four sections, corresponding to the four operation states transversed, with each one being labeled FF, TLs, TL or LL according to the respective operating mode. The transition to TLs occurs around 8 s and at 11.5 s the quadrotor stops sliding and enters the TL state. Finally, around 12 s the quadrotor has two points of contact with the ground and enters the LL state, completing the landing procedure.

With an eye on Figure 6 we can see the effects of the initial impact with the slope at the 8 s. The quadrotor starts an initial slide along the slope but looses velocity. This velocity is quickly recovered as the quadrotor tries to track

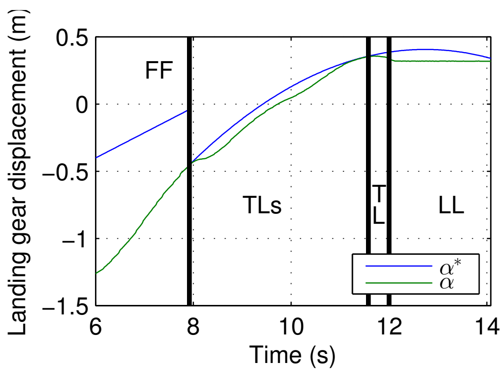

Fig. 6. Horizontal displacement along the slope.

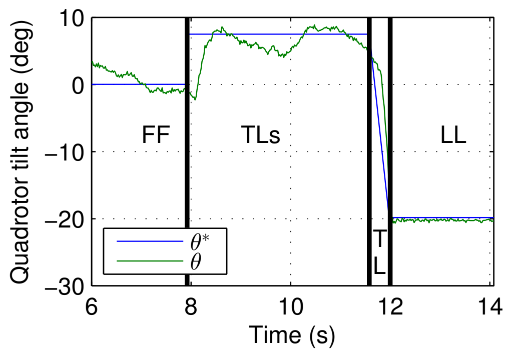

Fig. 7. Quadrotor tilt angle.

the desired maneuver. Finally, the quadrotor comes to a halt and a transition to TL occurs, with the landed state being attained shortly after. Despite all the uncertainties existing in the model, the controller proves to be robust and maintains the tracking error small.

Looking at Figure 7, we see the time evolution of of the quadrotor's tilt angle. In free flight the angle is approximately zero, as asserted in the reference maneuver discussion in Section IV-A.1. Once in TLs, the quadrotor tracks a reference maneuver where $\theta_0 = 7.5°$. This tilt angle is close enough to the initial angle and confers increased controllability to the quadrotor. Additionally, it helps to avoid a return to free flight situation, as could happen easily if the reference maneuver was defined with $\theta_0 = 0$. Once the TL state is entered, the quadrotor tries to follow a constant angular velocity trajectory that leads to all of the landing gear being in contact with the landing slope.

VI. Conclusions

This paper addressed the problem of robust landing control of a quadrotor UAV, considering explicitly the interaction with the ground, that guarantees successful maneuvers even in sloped terrains and in the presence of external disturbances and uncertain parameters. The vehicle was modeled as a hybrid automaton, whose states reflect the different dynamic behaviors exhibited by the UAV along the stages of the landing maneuver. The landing procedure was then cast as the problem of changing the operating mode of the vehicle from the initial to the final desired state, through the edge transitions allowed for the hybrid automaton. The transitions between intermediate operating modes were achieved through the application of low-level feedback controllers, associated with each mode, to track robust reference signals. A supervisor controller was designed to sense the current operation mode of the vehicle and choose the appropriate low-level controller and robust transition reference trajectory. The combined properties of the low-level controllers and reference trajectories ensures that the desired intermediate transitions are attained robustly with respect to uncertainties in the model and environment parameters and that the final desired state is reached. Experimental results using a small scale radio controlled quadrotor vehicle were presented to assess the feasibility of the proposed hybrid controller.

References

[1] K. Fregene (Guest Editor), "Unmanned aerial vehicle – special issue," *IEEE Control Systems Magazine*, vol. 32, no. 5, pp. 32–109, Oct. 2012.

[2] T. Hamel, R. Mahony, A. Tayebi (Eds.), "Aerial robotics [special issue]," *Control Engineering Practice*, vol. 18, no. 7, pp. 677–836, 2010.

[3] G. Zhou et al. (Ed.), "Special issue on unmanned airborne vehicle (uav) sensing systems for earth observations," *IEEE Transactions on Geoscience and Remote Sensing*, vol. 47, no. 3, march 2009.

[4] L. Marconi, A. Isidori, and A. Serrani, "Autonomous vertical landing on an oscillating platform: an internal-model based approach," *Automatica*, vol. 38, no. 1, pp. 21 – 32, 2002.

[5] B. Hérissé, T. Hamel, R. E. Mahony, and F.-X. Russotto, "Landing a vtol unmanned aerial vehicle on a moving platform using optical flow." *IEEE Transactions on Robotics*, pp. 77–89, 2012.

[6] H. Voos and H. Bou-Ammar, "Nonlinear tracking and landing controller for quadrotor aerial robots," in *Proceedings of the IEEE International Conference on Control Applications*, sept. 2010, pp. 2136 –2141.

[7] D. Mellinger, M. Shomin, and V. Kumar, "Control of quadrotors for robust perching and landing," *Proceedings of the International Powered Lift Conference*, 2010.

[8] A. Lussier Desbiens and M. R. Cutkosky, "Landing and perching on vertical surfaces with microspines for small unmanned air vehicles," *Journal of Intelligent and Robotic Systems*, vol. 57, no. 1-4, pp. 313–327, Jan. 2010.

[9] M. Fumagalli, R. Naldi, A. Macchelli, R. Carloni, S. Stramigioli, and L. Marconi, "Modeling and control of a flying robot for contact inspection," in *Proceedings of the IEEE/RSJ International Conference on Intelligent Robots and Systems*, Oct. 2012, pp. 3532–3537.

[10] D. Cabecinhas, R. Naldi, L. Marconi, C. Silvestre, and R. Cunha, "Robust take-off for a quadrotor vehicle," *IEEE Transactions on Robotics*, vol. 28, no. 3, pp. 734–742, 2012.

[11] A. Albers, S. Trautmann, T. Howard, T. A. Nguyen, M. Frietsch, and C. Sauter, "Semi-autonomous flying robot for physical interaction with environment," in *Proceedings of the IEEE Conference on Robotics Automation and Mechatronics*, 2010, pp. 441–446.

[12] L. Marconi and R. Naldi, "Control of aerial robots: Hybrid force and position feedback for a ducted fan," *Control Systems, IEEE*, vol. 32, no. 4, pp. 43 –65, aug. 2012.

[13] L. Marconi, R. Naldi, and L. Gentili, "A control framework for robust practical tracking of hybrid automata," in *Proceedings of the IEEE Conference on Decision and Control*, 2009, pp. 661–666.

[14] B. Brogliato, *Nonsmooth Mechanics Model, Dynamics and Control*. Springer, 1996.

[15] D. Cabecinhas, R. Cunha, and C. Silvestre, "Saturated output feedback control of a quadrotor aircraft," in *Proceedings of the American Control Conference*. IEEE, 2012, pp. 4667–4602.

[16] A. Isidori, *Nonlinear Control Systems II*. Springer Verlag London, 1999.

[17] Horizon hobby inc. [Online]. Available: http://www.bladehelis.com

[18] VICON. [Online]. Available: http://www.vicon.com